TELKOMNIKA Indonesian Journal of Electrical Engineering
Vol. 12, No. 11, November 2014, pp. 7659 ~ 7667
DOI: 10.11591/telkomnika.v12i11.6556

Evaluation of Speed and Torque Estimations for the EKF-based Direct Torque Control in Induction Machines

Ibrahim M. Alsofyani*, Nik Rumzi Nik Idris, Y.A. Alamri, Low Wen Yao, Sajjad A. Anbaran
Faculty of Electrical Engineering, Universiti Teknologi Malaysia
UTM Skudai 81310, Johor, Malaysia
*Corresponding author, e-mail: aslofyani2002@yahoo.com

Abstract

Accurate estimations of unmeasurable variables are required for increasing the performance of sensorless induction motor drives. This can be achieved if the required variables are accurately estimated with a well-established observer. The paper presents an extended Kalman filter- based direct torque control to investigate the estimations of speed and torque under challenging rotor and stator resistor and load variations at low and high speed regions. In all investigated scenarios, the speed and torque estimation showed good robustness against perturbations and their errors have remained within acceptable error bands.

Keywords*: direct torque control, EKF, induction motor, current model, estimated speed, estimated toque*

1. Introduction

Since the establishment of the direct torque control (DTC) for induction motors in the 1980's [1-2], it has received increasing attention for its improvement. Rotor speed information is not involved in the classical DTC strategy as the stator flux estimation is achieved using the voltage equation. Nevertheless, the knowledge of speed is required for the system control, though the stator flux estimation is performed totally based on voltage-based model. Thus, to guarantee high DTC performance, rotor speed is one of the essential variables that have to be either estimated or measured. It is a well- known fact; speed sensors require regular maintenance and increase the cost and size of drive systems. Similarly, problems occur for the flux measurement when Hall Effect transducers are utilized. Therefore, to enhance the dynamic performance of the overall system, observers are more preferred than transducers and sensors. The observer-based estimators [3-6] have the advantages of removing the open-loop integration, removing the sensitivity to the stator resistor variation, and improving the stator flux and torque estimation at low speed.

There are various improved observer strategies for the solution of zero/low speed problem which are implemented in different control techniques. For example, a sliding-mode current and flux estimator using a continuous technique in combination with the field oriented controlled system is addressed for obtaining the estimated information of speed and rotor resistance showing a good improvement in the control system [7]. Ref [8] describes an adaptive observer for simultaneous estimation of currents and rotor fluxes with adjusting the values of rotor and stator resistances by utilizing the information of a one stator current and speed knowledge. A combination of fuzzy logic and sliding mode control for model reference adaptive system (MRAS) is introduced in [9] for substituting the fixed-gain PI controller. The proposed complex MRAS-based estimation is said to accomplish a drive system improvement with the minimum speed range of 3 to 10.5 r/s.

An alternative to the previous deterministic studies, extended Kalman filter (EKF) based research works as in [10-12] have been addressed. The stochastic nature and high convergence rate of EKFs help to obtain highly accurate estimates of state variables under noisy conditions and overcome the uncertainties in the fundamental model of IMs [13]. Thus, EKF is considered to be less sensitive to the parameter variations especially if its covariance matrices are correctly selected. Among previous DTC with EKF-observer studies, ref [14]

Received August 13, 2014; Revised September 18, 2014; Accepted October 2, 2014

estimates the stator flux and rotor speed information along with stator and rotor resistor parameters. In spite of system improvement in different speed regions, the method requires very large executing time and causes the performance of EKF to deteriorate due to high number of estimated states [13].

This paper is aimed to combine EKF-based estimation algorithms with direct torque control for investigation of estimated speed and torque in different speed regions, incorporating zero speed operation. For this objective, unlike previous EKF-based observer studies, only five parameters are estimated using the optimization technique, as the performance of EKF relies on the optimized choice of its covariance matrices [13]. Additionally, the paper aims to highlight the performances of speed and torque under various resistor, load and speed conditions.

The paper is organized in five sections. The following section describes the extended Kalman filter algorithm. Section III presents the direct torque controller. Simulation results discussion are given in Sections IV. Finally, conclusion is given in V.

2. Extentded Kalman Filter Algorithm

In this study, EKF is used to concurrently estimate current, rotor flux, and rotor speed for speed sensorless control of IMs. However, the precise estimation of these state variables is very much reliant on how well the filter matrices are selected over a wide speed range [15]. The extended model to be used in the development of the EKF algorithm can be written in the following general form (as referred to the stator stationary frame.

$$\dot{x}_i(t) = f_i(x_i(t), u(t)) + w_i(t) \tag{1}$$

$$f_i(x_i(t), u(t)) = A_i(x_i(t))x_i(t) + Bu(t) \tag{2}$$

$$Y(t) = H_i(x_i(t))x_i(t) + Bu(t) + v_i(t) \tag{3}$$

$$\underbrace{\begin{bmatrix} \dot{i}_{sd} \\ \dot{i}_{sq} \\ \dot{\psi}_{rd} \\ \dot{\psi}_{rq} \\ \dot{\omega}_r \end{bmatrix}}_{\dot{X}} = \underbrace{\begin{bmatrix} -\left(\frac{R_s}{L_\sigma} + \frac{L_m^2 R_r}{L_\sigma L_r^2}\right) & 0 & \frac{L_m R_r}{L_\sigma L_r^2} & \frac{\omega_r L_m}{L_\sigma L_r} & 0 \\ 0 & -\left(\frac{R_s}{L_\sigma} + \frac{L_m^2 R_r}{L_\sigma L_r^2}\right) & -\frac{\omega_r L_m}{L_\sigma L_r} & \frac{L_m R_r}{L_\sigma L_r^2} & 0 \\ \frac{R_r}{L_r} & 0 & -\frac{R_r}{L_r} & -\omega_r & 0 \\ 0 & \frac{R_r}{L_r} L_m & \omega_r & -\frac{R_r}{L_r} & 0 \\ 0 & 0 & 0 & 0 & 0 \end{bmatrix}}_{A} \cdot \underbrace{\begin{bmatrix} i_{sd} \\ i_{sq} \\ \psi_{rd} \\ \psi_{rq} \\ \omega_r \end{bmatrix}}_{X} + \underbrace{\begin{bmatrix} 1/L_\sigma & 0 \\ 0 & 1/L_\sigma \\ 0 & 0 \\ 0 & 0 \\ 0 & 0 \end{bmatrix}}_{B} \cdot \underbrace{\begin{bmatrix} v_{sd} \\ v_{sq} \end{bmatrix}}_{u} + w(t) \tag{4}$$

$$\begin{bmatrix} i_{sd} \\ i_{sq} \end{bmatrix} = \underbrace{\begin{bmatrix} 1 & 0 & 0 & 0 & 0 \\ 0 & 1 & 0 & 0 & 0 \end{bmatrix}}_{H} \cdot \underbrace{\begin{bmatrix} i_{sd} \\ i_{sq} \\ \psi_{rd} \\ \psi_{rq} \\ \omega_r \end{bmatrix}}_{X} + v(t) \tag{5}$$

There i = 1, 2, extended state vector x_i is representing the estimated states, f_i is the nonlinear function of the states and inputs, A_i is the system matrix, u is the control-input vector, B is the input matrix, w_i is the process noise, H is the measurement matrix, and v_i is the measurement noise. The general form of IM can be represented by (4) and (5)

Where i_{sd} and i_{sq} are the d and q components of stator current, Ψ_{rd} and Ψ_{rq} are d-q rotor flux components, ω_r is the rotor electric angular speed in rad/s, v_{sd} and v_{sq} are the stator voltage components, L_s, $L_r$and L_m are the stator, rotor and mutual inductances respectively, R_s is the stator resistance, and R_r is the rotor resistance.

In this section, the EKF algorithm used in the IM model will be derived using the extended model in (4) and (5). For nonlinear problems, such as the one in consideration, the KF method is not strictly applicable, since linearity plays an important role in its derivation and performance as an optimal filter. The EKF technique attempts to overcome this difficulty by using a linearized approximation, where the linearization is performed about the current state estimate. This process requires the discretization of (4) and (5)—as follows-

$$\dot{x}_i(k+1) = f_i(x_i(k),u(k)) + w_i(k) \tag{6}$$

$$f_i(x_i(k),u(k)) = A_i(x_i(k))x_i(k) + Bu(k) \tag{7}$$

$$Y(k) = H_i(x_i(k))x_i(k) + Bu(k) + v_i(k) \tag{8}$$

The linearization of (7) is performed around the current estimated state vector $\hat{x}_i$ given as follows.

$$F_i(k) = \left.\frac{\partial f_i(x_i(k),u(k)}{\partial x_i(k)}\right|_{\hat{x}_i(k)} \tag{9}$$

The resulting EKF algorithm can be presented with the following recursive relations:

$$P(k) = F(k)P(k)F(k)^{-1} + Q \tag{10}$$

$$K(k+1) = H^T P(k)(HP(k+1)H^T + R)^{-1} \tag{11}$$

$$\hat{x}(k+1) = \hat{f}(x(k),u(k)) + K(k)(Y(k) - H\hat{x}(k)) \tag{12}$$

$$P(k+1) = (I - K(k+1)H)P(k) \tag{13}$$

In (10)-(13)Q is the covariance matrix of the system noise, namely, model error, R is the covariance matrix of the output noise, namely, measurement noise, and P are the covariance matrix of state estimation error. The algorithm involves two main stages: prediction and filtering. In the prediction stage, the next predicted states $\hat{f}(\cdot)$ and predicted state-error covariance matrices, $\hat{P}(\cdot)$ are processed, while in the filtering stage, the next estimated states $\hat{x}(k+1)$ obtained as the sum of the next predicted states and the correction term [second term in (12)], are calculated. The structure of the EKF algorithm is shown in Figure 1:

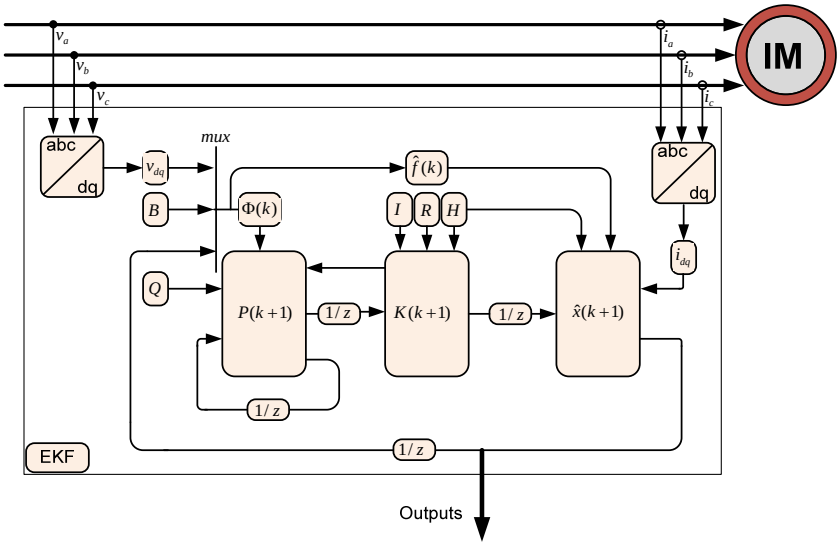

Figutre 1. Structure of Extended Kalman Filter

The electromagnetic torque based on EKF is expressed based on the selected state variables which are the stator current and rotor fluxr:

$$T_e = \frac{3}{2}\frac{p}{2}\frac{L_m}{L_r}\left(i_{sq}\psi_{dr} - i_{sd}\psi_{qr}\right) \tag{14}$$

The electromagnetic torque based on EKF is expressed based on the selected state variables which are the stator current and rotor fluxr:

3. Direct Torque Control

The DTC scheme, as initially proposed in [16], consists of a pair of hysteresis comparators, torque and flux calculator, a lookup table, and a voltage-source inverter. The control structure of DTC is much simpler than the FOC system due to the absence of frame transformer, pulse width modulator, and a position encoder. The decouple control of torque and flux is established by selecting appropriate voltage vectors to maintain the torque and flux errors within their hysteresis bands [16]. In DTC, the accuracy of the estimated stator flux is important to ensure correct voltage vector is selected for a decoupled torque and flux control.

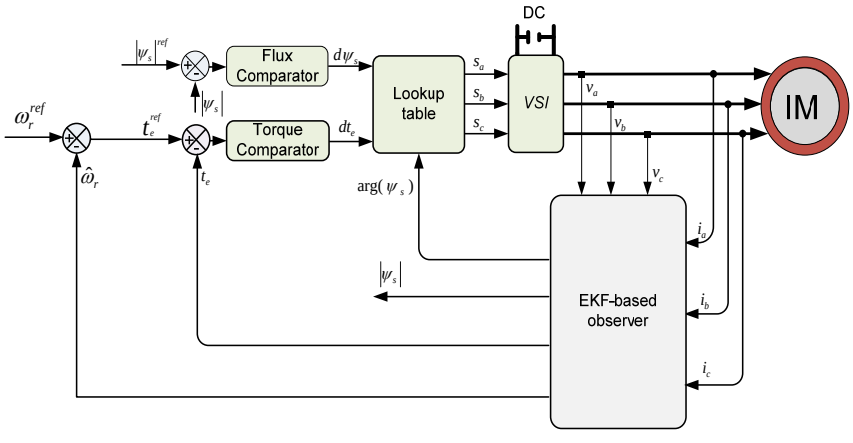

Figure 2. Complete EKF-based Direct Torque Control Scheme

From the estimated rotor speed and rotor flux linkage values using EKF filter, the stator flux can be achieved using the following equations.

$$\overline{\psi}_{sd} = \frac{L_m}{L_r}\overline{\psi}_{rd} + L_\sigma \bar{i}_{sd} \tag{15}$$

$$\overline{\psi}_{sq} = \frac{L_m}{L_r}\overline{\psi}_{rq} + L_\sigma \bar{i}_{sq} \tag{16}$$

After obtaining the stator flux information, the flux magnitude is subtracted with its reference value; its output is used in the flux comparator, whereas the angle is used for defining the voltage sector located in the lookup table as shown in Figure 2.

4. Simulation Results

To test the performance of rotor speed and electrical torque estimations for EKF-based direct torque control, investigations using the Matlab simulation are performed on an IM with with its rated values given in Table 1. Several tests are conducted, which impose challenging stator and rotor resistances, load torque, and rotor speed variations on the motor over a variety of speed regions. The EKF algorithm begins with initial state estimations of zero. The drive system along with the EKF observer is run in the sampling period of 2 μs.

The initial values of the error matrix *P* is started with the diagonal of one,. whereas covariance filters; *R* and *Q* in the EKF observer are established by using the genetic optimization algorithm [10] in order to obtain a quick convergence and to achieve the right transient- and steady-state performance. Therefore, the initial values for EKF filters are obtained in the following.

P = diag[1 1 1 1 1],
*Q = diag[2.68*10^{-10} 1.38*10^{-12} 6.25*10^{-14} 3.254*10^{-11} 1.37*10^{-2}],*
*and R=diag[3.1*10^{-3} 2.8*10^{-3}].*

Table 1. Induction Motor Parameters

R_s [Ω]	R_r [Ω]	L_s [H]	L_r [H]	L_m [H]	J_L [Kg. m^2]	p
3	4.1	0.5846	0.5937	0.5664	0.0031	4

The resulting performances are shown with the various changes of sp_m and sp_{es}, te_m and te_{es}, t_L, R_s, R_r, $e_{sp} = sp_m - sp_{es}$, and $e_{te} = te_m - te_{es}$, namely the measured and estimated speed, the measured and estimated electrical torque, load torque, stator resistor, rotor resistor, and estimation errors of speed and electrical torque, respectively. The estimated values can be seen in red, whereas the measured variables are shown in black.

In this experiment, the EKF-based DTC is investigated with the variations of load for high constant speed, as can be seen in Figure 3. Inspecting the results, it can be observed that, despite the switching causes of the load, the estimated information of speed and electrical torque follow their measured values more closely during the speed range within very low error bands. The measure of good EKF performance in the high speed region with load and no-load can be noted from the small error band of the estimated values. Additionally, it can be observed the proportional relationship between the electrical and load torques.

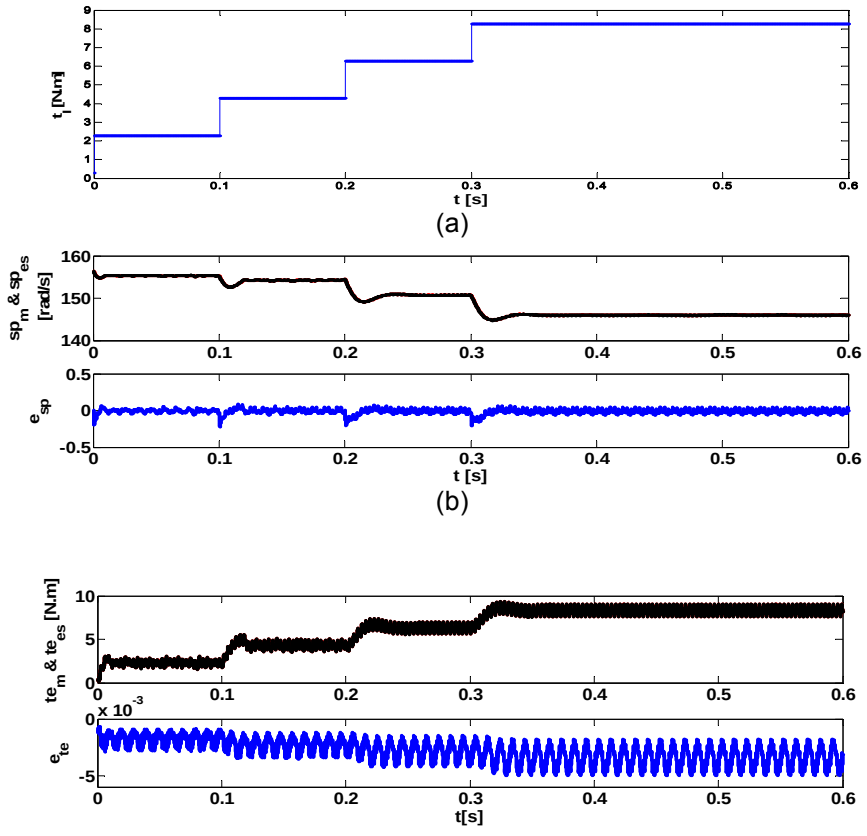

Figure 3. Simulation Results of EKF-based DTC for Load Torque Variation at High Steady Speed. (a) step-type load variation. (b) variations of sp_m , sp_{es} and e_{sp} . (c) variations of te_m, te_{es}, and e_{te}

It is essential to test the effect of motor parameter changes; due to temperature variations, on the performance of EKF observer. For this aim, the EKF-based DTC drive is tested for stator and rotor resistance variations while the IM is running at high speed (155 rad/s) under no-load. The stator resistance starts incrementing at 0.07 s by 0.5 ohm till it reaches 100% of the rated value at 0.59 s as shown in Figure 4. Similarly, with the same duration of high-speed operation, rotor resistance keeps incrementing by 0.667 ohm until it becomes doubled at 0.6 s as depicted in Figure 5. Inspecting the results in Figure 4 and 5, it can be seen that, the estimated speed for both stator and rotor resistor tests tracks the measured speed with gradual increase of the error. However, the error band remains reasonably within ±1 rad/s for both tests. It is also obvious that the measured speed, under rotor-test condition, diverge slightly from the estimated one, which makes the error moves in the negative direction. With regard to the torque estimation, the variations of stator resistor causes proportional increase in the torque error with less than -0.1 N.m., whereas, the electrical torque response towards the rotor resistance variations remains constant within smaller error band than that of the stator, indicating stator resistor still has smaller effect in the current model when compared with the voltage model.

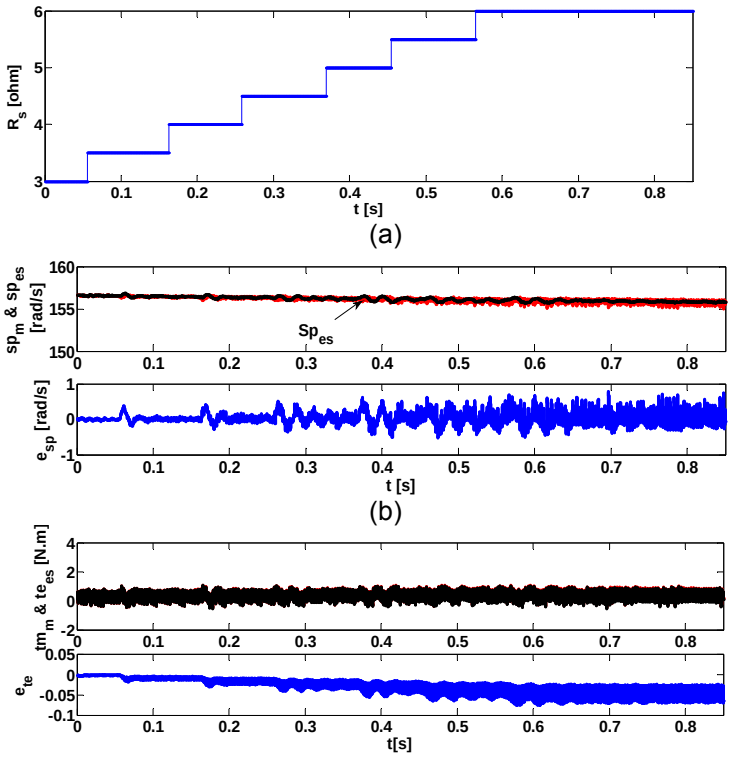

Figure 4. Simulation Results of EKF-based DTC for Stator Resistor Variation at High Steady Speed. (a) step-type stator resistor variation. (b) variations of sp_m , sp_{es} and e_{sp}. (c) variations of te_m, te_{es}, and e_{te}

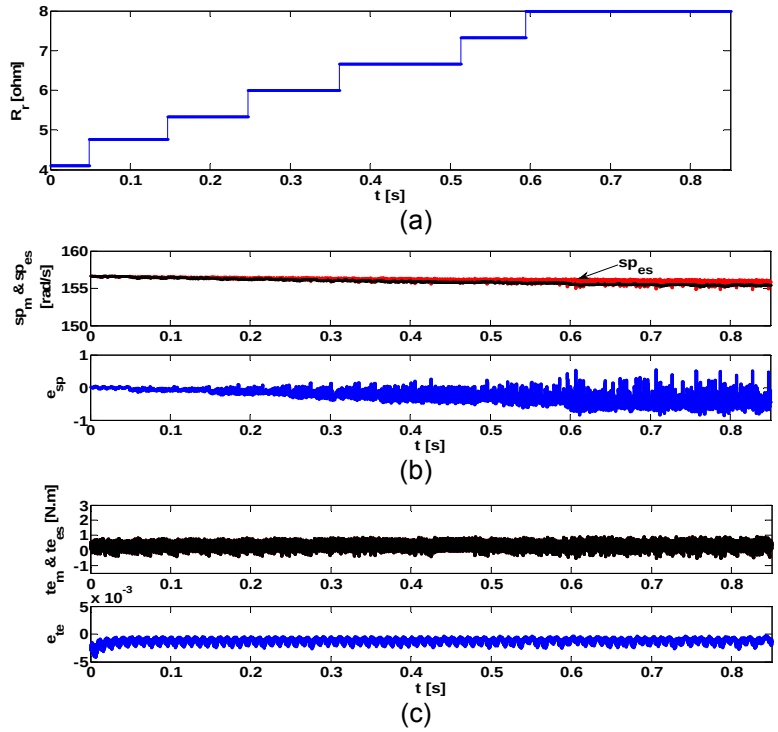

Figure 5. Simulation Results of EKF-based DTC for Rotor Resistor Variation at High Steady Speed. (a) step-type rotor resistor variation. (b) variations of sp_m , sp_{es} and e_{sp} . (c) variations of te_m, te_{es}, and e_{te}

The challenging scenario is presented in Figure 6 which shows the consecutive variations of three parameters; rotor and stator resistors and load torque at different low and middle speed regions. It is shown that the estimated and measured speeds are almost coincided at the steady state before rotor and stator increases except there is a slight error increase when load is introduced. By inspecting the results during the transient state, it is obvious that the error band is small within the interval before the introduction of resistor and load changes. With regard to the electrical torque, electrical torque error remains within small error band for all speed regions and for transient and steady states. It is noted that the electrical torque error is slightly affected after the rapid variation of load torque. Overall, the estimated speed and torque remained within acceptable error range, even though being under hindering conditions.

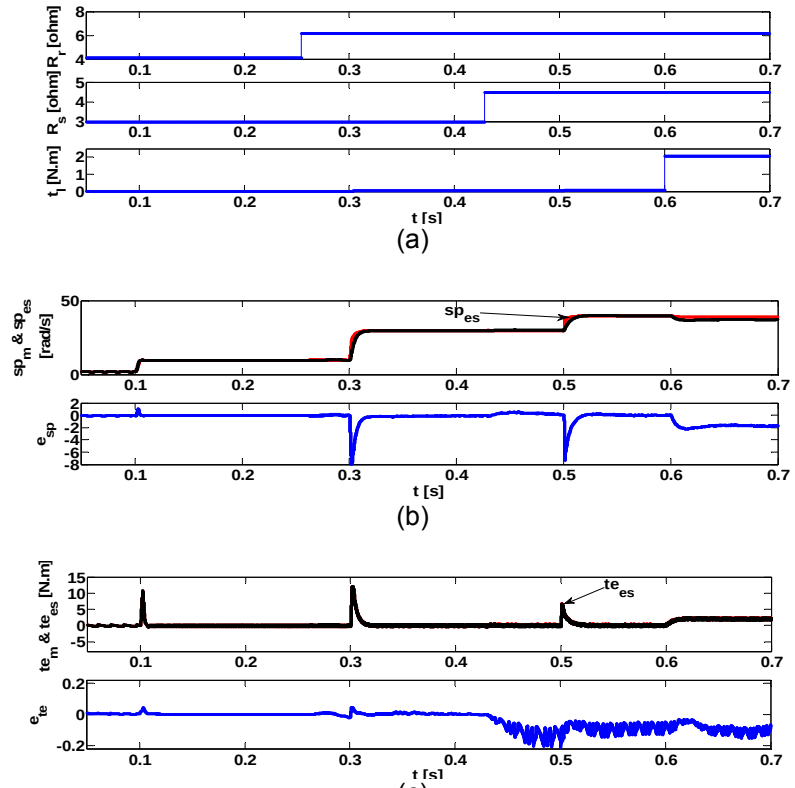

Figure 6. Simulation Results of EKF-based DTC for Load Torque, Rotor and Stator Resistor Variations at Different Low Speed Regions; (a) step-type rotor resistor variation. (b) variations of sp_m , sp_{es} and e_{sp} . (c) variations of te_m, te_{es}, and e_{te}.

4. Conclusion

In this paper, extended Kalman filter is proposed as a current model for direct torque control of induction motor. The EKF-based observer marks high improvement on direct torque control. Unlike previous studies, the focus of this work is on the evaluation of speed and torque estimations. The EKF-DTC drive has been tested for hindering variations of load torque, rotor and stator resistors at different speed regions, including zero speed operation. For all the results, torque and speed errors remained within a reasonable band even under very challenging conditions, signifying the good performance of the proposed technique.

References

[1] M Depenbrock. Direct self-control (DSC) of inverter-fed induction machine. *Power Electronics, IEEE Transactions on*. 1988; 3: 420-429.

[2] I Takahashi, T Noguchi. A New Quick-Response and High-Efficiency Control Strategy of an Induction Motor. *Industry Applications. IEEE Transactions on*. 1986; IA-22: 820-827.
[3] S Danan, L Wenli, D Lijun, L Zhigang. Speed Sensorless Induction Motor Drive Based on EKF and G-1 Model. *Computer Distributed Control and Intelligent Environmental Monitoring (CDCIEM), 2011 International Conference on*. 2011: 290-294.
[4] AV Ravi Teja, C Chakraborty, S Maiti, Y Hori. A New Model Reference Adaptive Controller for Four Quadrant Vector Controlled Induction Motor Drives. *Industrial Electronics, IEEE Transactions on*. 2012; 59: 3757-3767.
[5] Y Sayouti, A Abbou, M Akherraz, H Mahmoudi. *Sensor less low speed control with ANN MRAS for direct torque controlled induction motor drive*. Power Engineering, Energy and Electrical Drives (POWERENG), International Conference on. 2011: 1-5.
[6] SA Davari, DA Khaburi, W Fengxiang, RM Kennel. Using Full Order and Reduced Order Observers for Robust Sensorless Predictive Torque Control of Induction Motors. *IEEE Trans.,Power Electron.,* 2012; 27: 3424-3433.
[7] A Derdiyok. Speed-Sensorless Control of Induction Motor Using a Continuous Control Approach of Sliding-Mode and Flux Observer. *Industrial Electronics, IEEE Transactions on*. 2005; 52:1170-1176.
[8] FR Salmasi, TA Najafabadi. An Adaptive Observer With Online Rotor and Stator Resistance Estimation for Induction Motors With One Phase Current Sensor. *Energy Conversion, IEEE Transactions on*. 2011; 26: 959-966.
[9] SM Gadoue, D Giaouris, JW Finch. MRAS Sensorless Vector Control of an Induction Motor Using New Sliding-Mode and Fuzzy-Logic Adaptation Mechanisms. *IEEE Trans.,Ene. Conv.,* 2010; 25: 394-402.
[10] KL Shi, TF Chan, YK Wong, SL Ho. Speed estimation of an induction motor drive using an optimized extended Kalman filter. *IEEE Trans. Ind. Electron.,* 2002; 49: 124-133.
[11] IM Alsofyani, N Idris, T Sutikno, YA Alamri. An optimized Extended Kalman Filter for speed sensorless direct troque control of an induction motor. *IEEE Proc. PECon Conf.*, 2012: 319-324.
[12] IM Alsofyani, NRN Idris, M Jannati, SA Anbaran, YA Alamri. Using NSGA II multiobjective genetic algorithm for EKF-based estimation of speed and electrical torque in AC induction machines. *Power Engineering and Optimization Conference (PEOCO), IEEE 8th International*, 2014: 396-401.
[13] IM Alsofyani, NRN Idris. A review on sensorless techniques for sustainable reliablity and efficient variable frequency drives of induction motors. *Renewable and Sustainable Energy Reviews*. 2013; 24: 111-121.
[14] M Barut, R Demir, E Zerdali, R Inan. Speed-sensorless direct torque control system using Bi-input extended Kalman filter for induction motors. *Electrical Machines and Power Electronics and 2011 Electromotion Joint Conference (ACEMP), International Aegean Conference on*. 2011: 343-346.
[15] S Buyamin,JW Finch. Comparative Study on Optimising the EKF for Speed Estimation of an Induction Motor using Simulated Annealing and Genetic Algorithm. *IEEE Proc. IEMDC Conf.,* 2007: 1689-1694.
[16] NRN Idris, AHM Yatim. Direct torque control of induction machines with constant switching frequency and reduced torque ripple. *IEEE Trans. Ind. Electron.,* 2004; 51: 758-767.